Acta Cryst. (1983). A**39**, 257–268

The Relation of the Stress Dependence of $|F(\mathbf{H})|^2$ to Inner Compliance and Internal Strain Tensors in 20 Simple Crystal Structures

BY C. S. G. COUSINS

Physics Department, University of Exeter, Stocker Road, Exeter, Devon EX4 4QL, England

(*Received* 24 *June* 1982; *accepted* 2 *November* 1982)

Abstract

Internal strain tensors describe the relative displacements of sublattices in stressed crystals in which some atoms occupy sites lacking inversion symmetry. The variation of $|F(\mathbf{H})|^2$ in such crystals is shown to depend on *inner compliance tensors* which are essentially products of internal strain tensors with the macroscopic elastic compliance tensor. The forms of the inner compliance tensors and the uniaxial stress derivatives of $|F(\mathbf{H})|^2$ are tabulated for 20 simple crystal structures in which the number of atoms per lattice point is 2, 3 or 4.

Introduction

In connection with the formal expression of inner elasticity (Cousins, 1978*a*,*b*) a programme of measurement of internal strain tensors has been recently begun (Cousins, Gerward, Nielsen, Staun Olsen, Selsmark, Sheldon & Webster, 1982; Cousins, Gerward, Staun Olsen, Selsmark & Sheldon, 1982).

In this paper a systematic examination of the simplest crystal structures with 2, 3 or 4 atoms per lattice point is presented with the aim of simplifying the selection of which diffraction peaks should be observed (as functions of uniaxial stress) if full sets of internal strain components are to be obtained. These results cover the structures where measurements on a limited number of selected reflections will provide sufficient information. If there are more than four atoms per lattice point the measurement of a large number of reflections will almost certainly be needed.

An account of internal strain is given in § 2. It is similar to, but an improvement on, the earlier discussion (Cousins, 1978*a*). In § 3 the formal results for the dependence of $|F(\mathbf{H})|^2$ on stress are derived for the general case and are then specialized to the case of uniaxial stress. Whilst these formal results apply equally to simple and complex structures no examples of the latter are discussed here.

Inner compliance tensors prove to be the key quantities determining the effect of stress on $|F(\mathbf{H})|^2$. They are introduced by § 4 and the major part of this section is devoted to the symmetry analysis of these tensors for 20 different simple crystal structures. The results are presented in tables. It is also shown how the internal strain tensors may be subsequently retrieved provided the elastic stiffness tensor for the crystal is known.

In § 5 the stress dependence of $|F(\mathbf{H})|^2$ is tabulated for the 20 structures under discussion.

0567-7394/83/020257-12$01.50

2. Relative displacement, inner displacement and internal strain

2.1. *Condition for occurrence of relative displacement*

If each lattice point in a crystal structure is associated with n distinguishable material units (atoms, ions, *etc.*) then the crystal can be considered as n interpenetrating identical sublattices $L_1, L_2, \ldots, L_n$. Every site on a given sublattice has the same symmetry but different sublattices may have different symmetries. The group of point operations that embodies the symmetry of the environment of sites on L_α will be denoted by G_α. Compatibility with translational periodicity constrains G_α to be one of the 32 point groups normally encountered in crystal classification.

The occurrence of relative displacement can be illustrated by reference to Fig. 1 which shows schematically the effect of a homogeneous deformation, represented by the matrix J, on two sublattices L_α and L_β. Fig. 1(*a*) is the situation before the deformation J is applied and Fig. 1(*b*) shows what happens when both G_α and G_β contain the inversion. The crucial role of the inversion is easily appreciated: if it is present in G_α then the equivalence of the vectors $\mathbf{r}$ and $-\mathbf{r}$ with respect to any site on L_α prevents the atom at such a site from being preferentially displaced asymmetrically with respect to the environment. The same argument applies to the atoms on L_β. Since the atoms on L_α are part of the environment of those on L_β and conversely, it is a necessary condition for the occurrence of relative displacement that at least one of G_α and G_β should lack the inversion. Fig. 1(*c*) shows the situation when such relative displacement occurs.

Vectors between lattice points on L_α and L_β change under the homogeneous deformation according to

$$\mathbf{r}^{\alpha\beta} = J\mathbf{r}_0^{\alpha\beta} + \boldsymbol{\delta}^{\alpha\beta}, \tag{1}$$

where $\boldsymbol{\delta}^{\alpha\beta} = 0$ if $\alpha = \beta$ or if G_α and G_β both contain the inversion.

Suppose that n_i sites possess inversion symmetry. Then there will be $(m - 1)m/2$ distinct vectors $\boldsymbol{\delta}^{\alpha\beta}$ where $m = n$ if $n_i = 0$ or 1 whilst $m = n - n_i + 1$ if $n_i \geq 2$. Of these vectors $m - 1$ at most can be independent and it is essential for the relative displacement vectors to be defined in a systematic way permitting easy enumeration. A system shown schematically in Figs. 2(*a*) and (*b*) proves satisfactory in this respect. It avoids some confusion if the two cases $m = n$ and $m \neq n$ are treated separately and we begin with the former. A row of n points, corresponding to the sublattice indices α, are numbered consecutively. If $n_i = 1$ the site with inversion is the nth point. The straight links between adjacent points represent the vectors $\boldsymbol{\delta}^\lambda$ where λ, an interlattice index running from 1 to $(n - 1)n/2$, has been introduced to reduce the number of superscripts and to emphasize the shift from a sublattice approach to an interlattice one. Each of these links corresponds to a possibly independent $\boldsymbol{\delta}^\lambda$. The sense of the $\boldsymbol{\delta}^\lambda$ is chosen so that the vector represents the relative displacement of the sublattice of higher index with respect to the one of lower index. A second row of $n - 2$ links joins pairs of points separated by an intervening point and represents the vectors $\boldsymbol{\delta}^n$ to $\boldsymbol{\delta}^{2n-3}$. This procedure is continued until the $(n - 1)$th row where there is a final link between the first and last points representing $\boldsymbol{\delta}^{n(n-1)/2}$.

The relation of dependence is clear: the vector represented by the pth link in the qth row is equal to the sum of the vectors between the sublattice points p and $p + q$. The interlattice index is given by

$$\pi = p + \tfrac{1}{2}(q - 1)(2n - q)$$

and

$$\boldsymbol{\delta}^\pi = \sum_{\lambda=p}^{p+q-1} \boldsymbol{\delta}^\lambda. \tag{2a}$$

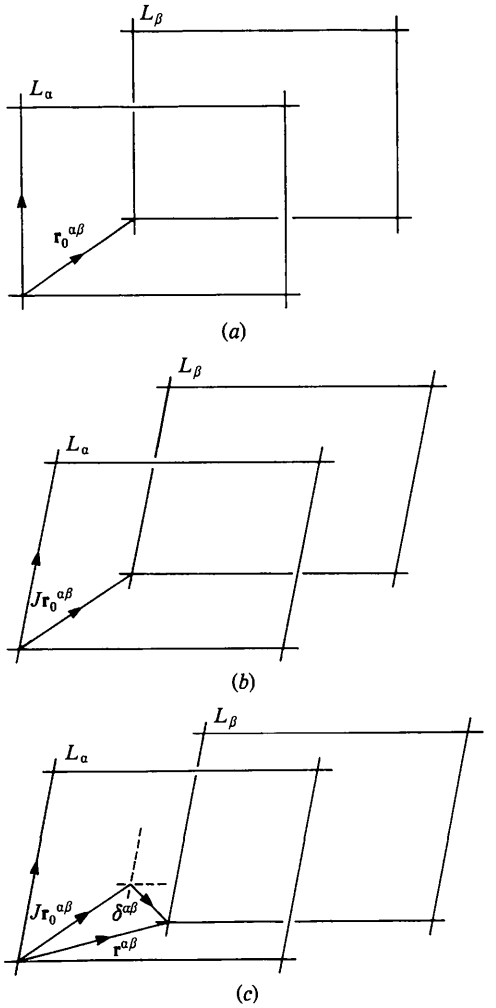

Fig. 1. The relative displacement of two sublattices. In (*a*) the interlattice vector $\mathbf{r}_0^{\alpha\beta}$ is shown in the undeformed state. In (*b*) the interlattice vector has become $J\mathbf{r}_0^{\alpha\beta}$ due to uniform deformation in a situation where both sublattices have inversion symmetry. In (*c*) at least one sublattice lacks the inversion and relative displacement $\boldsymbol{\delta}^{\alpha\beta}$ occurs.

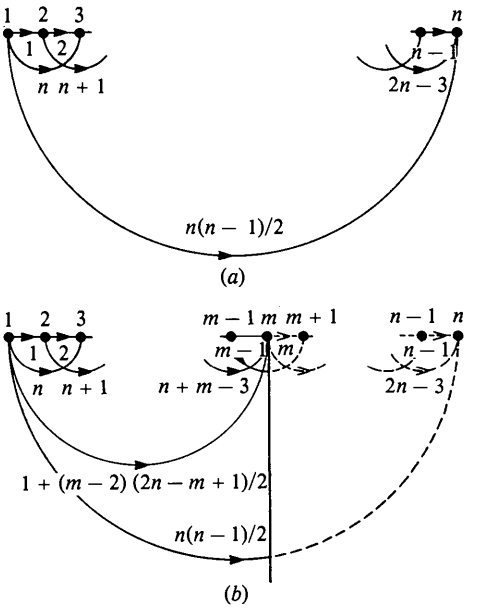

Fig. 2. Assignment of sublattice and interlattice indices. The numbers above the points are sublattice indices and those on the links are interlattice indices. Indices corresponding to sites with inversion symmetry, if any, are placed on the right. If n_i is the number of such sites then (*a*) illustrates $n_i = 0$ or 1 in which case $m = n$ and (*b*) illustrates $n_i \geq 2$ in which case $m = n - n_i + 1 < n$. Other details are explained in § 2.1.

From the scheme of Fig. 2(*a*) this last relation may be written alternatively in the form

$$\boldsymbol{\delta}^{\pi} = \boldsymbol{\delta}^{\lambda}\, l^{\lambda\pi} \tag{2b}$$

where λ runs from 1 to $n-1$ and $l^{\lambda\pi} = 1$ if 'λ lies in the loop of π' and is zero otherwise.

The case of $m \neq n$ is illustrated in Fig. 2(*b*). The construction of the diagram is broadly as before. All sites with inversion symmetry are placed on the right and a vertical line has been drawn down from the first of these, which corresponds to sublattice m. Links exclusively to the right of the vertical line are shown dotted and correspond to zero relative displacements. The $m(m-1)/2$ links exclusively to the left correspond to non-zero displacements. Links that cross the line are shown partly dotted and are equivalent to links with the same starting point but terminating at point m.

If $n_i \geq 1$ the number of sites lacking inversion is necessarily even and m is thus odd. The maximum number of independent $\boldsymbol{\delta}^{\lambda}$ is thereby reduced to $(m-1)/2$.

2.2. *Rotationally invariant parameters of inner displacement*

Although the matrix J and $m-1$ vectors $\boldsymbol{\delta}^{\lambda}$ completely specify the deformed lattice they are not suitable parameters for thermodynamic purposes. This is because a rigid rotation R following J turns J into RJ and $\boldsymbol{\delta}^{\lambda}$ into $R\boldsymbol{\delta}^{\lambda}$, but does not alter the strain energy. The problem is circumvented by defining the finite strain matrix η and $m-1$ vectors $\boldsymbol{\zeta}^{\lambda}$ by means of

$$I + 2\eta = \tilde{J}J \tag{3}$$

and

$$\boldsymbol{\zeta}^{\lambda} = \tilde{J}\boldsymbol{\delta}^{\lambda} \quad \lambda = 1, 2, \ldots, m-1, \tag{4}$$

where the tilde denotes transposition. If $n_i \geq 2$ (*i.e.* there are two or more sites with inversion symmetry) then

$$\boldsymbol{\zeta}^{\lambda} = 0, \quad \lambda = m, m+1, \ldots, n-1. \tag{5}$$

The remaining $\boldsymbol{\zeta}^{\pi}$ are defined by

$$\boldsymbol{\zeta}^{\pi} = \boldsymbol{\zeta}^{\lambda}\, l^{\lambda\pi}, \quad \pi = n, n+1, \ldots, n(n-1)/2 \tag{6}$$

using the prescription of § 2.1. Rotational invariance for the inner displacement vectors $\boldsymbol{\zeta}^{\pi}$ is assured because $\tilde{R}R = I$ for a rigid rotation.

2.3. *Internal strain tensors*

Since the inner displacement is the crystal response to the imposition of finite strain each inner displacement vector can be expressed as a Taylor series in the components of the finite strain matrix:

$$\zeta_i^{\lambda} = A_{ijk}^{\lambda}\,\eta_{jk} + \tfrac{1}{2}A_{ijklm}^{\lambda}\,\eta_{jk}\,\eta_{lm} + \ldots, \quad \lambda = 1, 2, \ldots, m-1, \tag{7}$$

where there is no constant term since $\boldsymbol{\zeta}^{\lambda} = 0$ when $\eta = 0$. The coefficients A_{ijk}^{λ} and A_{ijkim}^{λ} are components of the internal strain tensors. Since η is symmetric the usual Voigt contraction of suffixes and the conventional modifications of magnitude may be employed ($\eta_{11} \rightarrow \eta_1$, $\eta_{23} = \eta_{32} \rightarrow \tfrac{1}{2}\eta_4$, *etc.*) and the above equation re-written as

$$\zeta_i^{\lambda} = A_{iJ}^{\lambda}\,\eta_J + \tfrac{1}{2}A_{iJK}^{\lambda}\,\eta_J\,\eta_K + \ldots, \quad \lambda = 1, 2, \ldots, m-1, \tag{8}$$

where $A_{ijk}^{\lambda} \rightarrow A_{iJ}^{\lambda}$ without change of magnitude.

It can be shown (Cousins, 1978*a*) that the second term on the right of (8) has no effect on the elasticity of the crystal below the fourth order and may be ignored. We are left with up to $m-1$ independent internal strain tensors defined by

$$\zeta_i^{\lambda} = A_{iJ}^{\lambda}\,\eta_J, \quad \lambda = 1, 2, \ldots, m-1 \tag{9}$$

and, by invoking (6), a number of dependent ones defined by

$$A_{iJ}^{\pi} = A_{iJ}^{\lambda}\, l^{\lambda\pi}, \quad \pi = n, n+1, \ldots, n(n-1)/2, \tag{10}$$

where λ is summed 1 to $m-1$ and where, again, if $n_i \geq 2$

$$A_{iJ}^{\lambda} = 0, \quad \lambda = m, m+1, \ldots, n-1. \tag{11}$$

The effect of symmetry on the components of the internal strain tensors is fully covered by Cousins (1978*b*) and illustrated for corundum by Cousins (1981). When such an analysis has been completed for a given crystal structure a further simplification may be obtained as a result of geometrical conditions embodied by (10) and (11) and illustrated in Fig. 2.

3. Effect of relative displacement on $|F(\mathbf{H})|^2$ in a homogeneously deformed crystal

3.1. *General considerations*

Consider an unstrained crystal with n atoms or ions per lattice point at position $\mathbf{x}^{\alpha}$, $\alpha = 1, 2, \ldots, n$. The structure factor for Bragg diffraction from planes whose reflection vector is $\mathbf{H}$ is then

$$F(\mathbf{H}) = \sum_{\alpha=1}^{n} f_{\alpha}(\theta,\lambda)\exp(i2\pi\mathbf{H}.\mathbf{x}^{\alpha}) \tag{12}$$

so that

$$|F(\mathbf{H})|^2 = \sum_{\alpha=1}^{n}\{f_{\alpha}(\theta,\lambda)\}^2 + \sum_{\alpha=1}^{n}\sum_{\beta=1}^{n}{}' f_{\alpha}(\theta,\lambda)\,f_{\beta}(\theta,\lambda) \times \exp[i2\pi\mathbf{H}.(\mathbf{x}^{\beta} - \mathbf{x}^{\alpha})], \tag{13}$$

where $f_{\alpha}(\theta,\lambda)$ is the scattering factor for radiation of wavelength λ for atom/ion α through 2θ, θ is the Bragg angle and the prime on the double summation indicates that terms in which $\alpha = \beta$ have been treated separately.

We now introduce the interlattice index π [running from 1 to $n(n-1)/2$ as in § 2.1] and write

$$|F(\mathbf{H})|^2 = \sum_{\alpha=1}^{n} \{f_\alpha(\theta,\lambda)\}^2 + 2 \sum_{\pi=1}^{n(n-1)/2} g_\pi(\theta,\lambda) \cos[2\pi \mathbf{H}.(\Delta\mathbf{x})^\pi], \quad (14)$$

where $(\Delta\mathbf{x})^\pi \equiv \mathbf{x}^\beta - \mathbf{x}^\alpha$ and $g_\pi(\theta,\lambda) \equiv f_\alpha(\theta,\lambda) f_\beta(\theta,\lambda)$.

Suppose now that the crystal is homogeneously deformed so that $\mathbf{x}^\alpha$ becomes $\mathbf{x}'^\alpha$ *etc.* and $\mathbf{H}$ becomes $\mathbf{H}'$. By (1) we have

$$(\Delta\mathbf{x}')^\pi = J(\Delta\mathbf{x})^\pi + \boldsymbol{\delta}^\pi \quad (15)$$

and, because $\mathbf{H}$ belongs to the reciprocal lattice,

$$\mathbf{H}' = \tilde{J}^{-1}\mathbf{H}. \quad (16)$$

The principal quantities affecting the intensity as a result of structure-factor variation are the arguments of the cosine in (14). These phases will be denoted by $\chi_{\mathbf{H}}^\pi$. Using (3), (4), (15) and (16) we obtain

$$\chi_{\mathbf{H}}'^\pi \equiv 2\pi\mathbf{H}'.(\Delta\mathbf{x}')^\pi = 2\pi\mathbf{H}.(\Delta\mathbf{x})^\pi + 2\pi\mathbf{H}(I+2\eta)^{-1}A^\pi\eta$$

or

$$\chi_{\mathbf{H}}'^\pi = \chi_{\mathbf{H}}^\pi + \psi_{\mathbf{H}}^\pi, \quad (17)$$

where, on introducing contracted tensor notation, the change of phase

$$\psi_{\mathbf{H}}^\pi = 2\pi H_i (I+2\eta)^{-1}_{ij} A^\pi_{jJ}\eta_J. \quad (18)$$

Since this is already a small quantity on account of the factor η_J we can replace $(I+2\eta)^{-1}$ by the identity matrix. Furthermore, the finite strain is related to the thermodynamic tension t through the compliance matrix S by $\eta_J = S_{JK}t_K$. In the limit of small stresses the thermodynamic tension is just the applied stress σ so (18) reduces to

$$\psi_{\mathbf{H}}^\pi = 2\pi H_i A^\pi_{iJ} S_{JK}\sigma_K. \quad (19)$$

The equivalent of (14) for the stressed crystal is thus

$$|F(\mathbf{H})|^2 = \sum_{\alpha=1}^{n} \{f_\alpha(\theta,\lambda)\}^2 + 2 \sum_{\pi=1}^{n(n-1)/2} g_\pi(\theta,\lambda)\cos(\chi_{\mathbf{H}}^\pi + \psi_{\mathbf{H}}^\pi). \quad (20)$$

Absolute changes in $|F(\mathbf{H})|^2$ are given by the difference between (20) and (14):

$$\Delta|F(\mathbf{H})|^2 = 2\sum_{\pi=1}^{n(n-1)/2} g_\pi(\theta,\lambda)\,[\cos(\chi_{\mathbf{H}}^\pi + \psi_{\mathbf{H}}^\pi) - \cos\chi_{\mathbf{H}}^\pi], \quad (21)$$

which, since $\psi_{\mathbf{H}}^\pi$ is small, reduces to

$$\Delta|F(\mathbf{H})|^2 = -\sum_{\pi\in\{\pi^*\}} g_\pi(\theta,\lambda)\,[2\psi_{\mathbf{H}}^\pi \sin\chi_{\mathbf{H}}^\pi + (\psi_{\mathbf{H}}^\pi)^2\cos\chi_{\mathbf{H}}^\pi], \quad (22)$$

where $\{\pi^*\}$ is the set of π values for which the A^π do not vanish. The smallness of $\psi_{\mathbf{H}}^\pi$ leads to further simplification. If there is one value of π in $\{\pi^*\}$ for which $\sin\chi_{\mathbf{H}}^\pi \neq 0$ then (22) becomes essentially linear in $\psi_{\mathbf{H}}^\pi$:

$$\Delta|F(\mathbf{H})|^2 = -2\sum_{\pi\in\{\pi^{**}\}} g_\pi(\theta,\lambda)\,\psi_{\mathbf{H}}^\pi \sin\chi_{\mathbf{H}}^\pi, \quad (23)$$

where $\{\pi^{**}\}$ is the subset of $\{\pi^*\}$ for which $\sin\chi_{\mathbf{H}}^\pi \neq 0$. If $\{\pi^{**}\}$ is an empty set then (22) becomes

$$\Delta|F(\mathbf{H})|^2 = -\sum_{\pi\in\{\pi^*\}} g_\pi(\theta,\lambda)(\psi_{\mathbf{H}}^\pi)^2\cos\chi_{\mathbf{H}}^\pi. \quad (24)$$

3.2. *Uniaxial stress dependence of* $|F(\mathbf{H})|^2$

If the stress is uniaxial with axis $[l_1 l_2 l_3]$ and of magnitude σ (positive for tensile stress) we may write $\sigma_K = \Lambda_K\sigma$ where $\Lambda_K = l_i l_j$, K being the Voigt contraction of ij. Equation (19) thus gives

$$\frac{\partial\psi_{\mathbf{H}}^\pi}{\partial\sigma} \equiv \frac{\psi_{\mathbf{H}}^\pi}{\sigma} = 2\pi H_i A^\pi_{iJ} S_{JK}\Lambda_K \quad (25)$$

and the stress derivatives of (23) and (24) are

$$\frac{\partial|F(\mathbf{H})|^2}{\partial\sigma} = -\frac{2}{\sigma}\sum_{\pi\in\{\pi^{**}\}} g_\pi(\theta,\lambda)\,\psi_{\mathbf{H}}^\pi \sin\chi_{\mathbf{H}}^\pi \quad (26)$$

and

$$\frac{\partial|F(\mathbf{H})|^2}{\partial\sigma} = -\frac{2}{\sigma}\sum_{\pi\in\{\pi^*\}} g_\pi(\theta,\lambda)(\psi_{\mathbf{H}}^\pi)^2\cos\chi_{\mathbf{H}}^\pi. \quad (27)$$

4. The inner compliance $\mathcal{E}^\pi$

Equations (23) and (24) show that the stress-induced changes in $|F(\mathbf{H})|^2$ are given by linear combinations of $\psi_{\mathbf{H}}^\pi$ or $(\psi_{\mathbf{H}}^\pi)^2$. Let us take (19) for the change of relative phase and express it as a matrix product for the general case of triclinic symmetry:

$$\psi_{\mathbf{H}}^\pi = 2\pi[h_1 h_2 h_3] \begin{bmatrix} \bar{A}^\pi_{11} & \bar{A}^\pi_{12} & \bar{A}^\pi_{13} & \bar{A}^\pi_{14} & \bar{A}^\pi_{15} & \bar{A}^\pi_{16} \\ \bar{A}^\pi_{21} & \bar{A}^\pi_{22} & \bar{A}^\pi_{23} & \bar{A}^\pi_{24} & \bar{A}^\pi_{25} & \bar{A}^\pi_{26} \\ \bar{A}^\pi_{31} & \bar{A}^\pi_{32} & \bar{A}^\pi_{33} & \bar{A}^\pi_{34} & \bar{A}^\pi_{35} & \bar{A}^\pi_{36} \end{bmatrix} \times \begin{bmatrix} S_{11} & S_{12} & S_{13} & S_{14} & S_{15} & S_{16} \\ S_{12} & S_{22} & S_{23} & S_{24} & S_{25} & S_{26} \\ S_{13} & S_{23} & S_{33} & S_{34} & S_{35} & S_{36} \\ S_{14} & S_{24} & S_{34} & S_{44} & S_{45} & S_{46} \\ S_{15} & S_{25} & S_{35} & S_{45} & S_{55} & S_{56} \\ S_{16} & S_{26} & S_{36} & S_{46} & S_{56} & S_{66} \end{bmatrix} \begin{bmatrix} \sigma_1 \\ \sigma_2 \\ \sigma_3 \\ \sigma_4 \\ \sigma_5 \\ \sigma_6 \end{bmatrix}, \quad (28)$$

where the definitions $\mathbf{h} \equiv a\mathbf{H}$ and $\bar{A}^\pi \equiv (1/a)A^\pi$ remove compensating dimensional factors from two of the matrices. The properties of the crystal determine the

central product $\bar{A}^\pi S$. From diffraction experiments we expect to obtain the components of these (3 × 6) matrices, which we shall call inner compliances and denote by Σ^π, where

$$\Sigma^\pi_{IK} \equiv \bar{A}^\pi_{IJ} S_{JK}. \tag{29}$$

When all the Σ^π_{IK} have been found the reduced internal strain components $\bar{A}^\pi_{IJ}$ may be retrieved through the use of the elastic stiffness matrix C *via*

$$\bar{A}^\pi_{IJ} = \Sigma^\pi_{IK} C_{KJ} \tag{30}$$

since $S_{JK} C_{KL} = \delta_{JL}$.

The point symmetry of $\bar{A}^\pi$ is the same as that of $(\Delta\mathbf{x})^\pi$ and is thus a subgroup of the Laue group. This means that Σ^π has the same symmetry as $\bar{A}^\pi$. In Table 1 are shown the non-zero components of $\bar{A}^\pi$, taken from Cousins (1978*b*, Table 10) and of S_{JK}, taken from Nye (1957). It will be noted from the Table that whilst Σ^π has the same form as $\bar{A}^\pi$ for a particular point group, there are certain differences between the relations of dependence between the components of $\bar{A}^\pi$ in trigonal and certain hexagonal classes and the corresponding relations in Σ^π. The difference is a factor of 2 that occurs in the Σ^π relations but not in the $\bar{A}^\pi$ relations. The reason is that $\bar{A}^\pi$ relates a vector (ζ^π) to the contracted form of a second-order tensor (η) in which *conventional* changes of magnitude have been made ($\eta_{23} \rightarrow \frac{1}{2}\eta_4$ *etc.*), whereas Σ^π relates ζ^π to a second-order tensor (σ) in which *no* such changes have been made.

Sometimes the symmetry elements pertaining to $\bar{A}^\pi$ and Σ^π will not be in the standard settings assumed in Table 1. In these cases the tensor transformation law will have to be applied in order to get the components appropriate to the variant setting (Cousins, 1978*b*, § 4). The fact that the $\bar{A}^\pi$ and Σ^π tensors conform to symmetry considerations and have the forms appropriate to certain point groups does not preclude further simplifications (vanishing of elements or additional relations) following from the geometrical dependence mentioned in § 2.3.

Table 1. *Forms of the tensors $\bar{A}^\pi$ and Σ^π for standard settings of the different point groups and of S for different Laue groups*

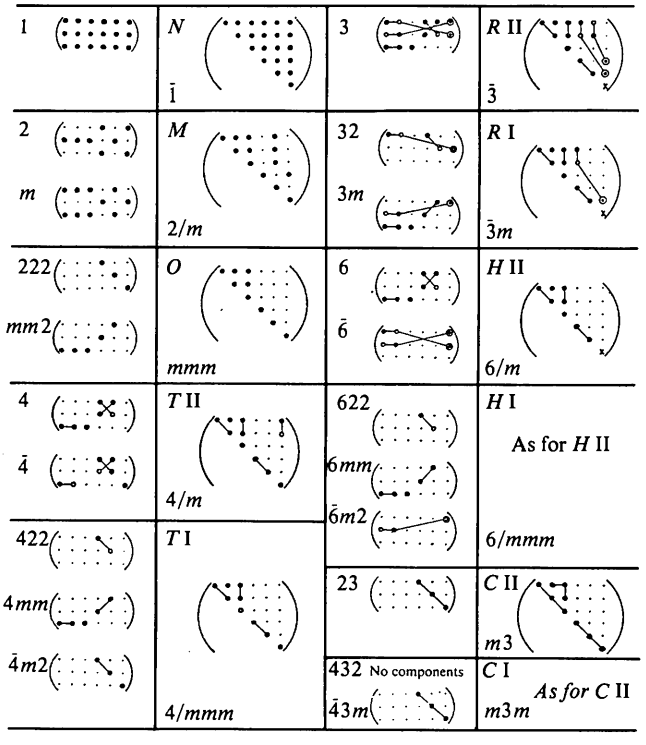

Notation: · zero component; ● non-zero component; ●——● equal components; ●——○ equal and opposite components; ⊙ in $\bar{A}^\pi$ equals ○ component to which it is joined; ⊙ in Σ^π equals twice the ○ component to which it is joined; ⊙ in S equals twice the ● component to which it is joined; × in S indicates that $S_{66} = 2(S_{11} - S_{12})$.

4.1. *Application to specific structures*

Twenty structures have been chosen to illustrate the cases m = 2, 3 and 4. They were taken from Slater (1965) and Galasso (1970). Table 2 contains information on these structures and indicates how sublattice indices have been assigned to atomic positions. These positions are given in order from lowest to

Table 2. *Allocation of sublattice indices to atomic positions in* 20 *crystal structures*

Structure	Space group	Sublattice indices 1	2	3	4
		Allocated to atomic positions			
$m = 2\ n = 2$					
Diamond	$Fd3m$	000	$\frac{1}{4}\frac{1}{4}\frac{1}{4}$		
Zincblende	$F\bar{4}3m$	000	: $\frac{1}{4}\frac{1}{4}\frac{1}{4}$		
HCP	$P6_3/mmc$	$\frac{1}{3}\frac{2}{3}\frac{1}{4}$	$\frac{2}{3}\frac{1}{3}\frac{3}{4}$		
Tungsten carbide	$P\bar{6}m2$	$\frac{1}{3}\frac{2}{3}\frac{1}{2}$	: 000		
White tin	$I4_1/amd$	000	$0\frac{1}{2}\frac{1}{4}$		
α-Uranium	$Cmcm$	$0v\frac{1}{4}$	$0\bar{v}\frac{3}{4}$		
Arsenic	$R\bar{3}m$	$00w$	$00\bar{w}$		
$m = 3\ n_t = 1\ n = 3$					
Fluorite	$Fm3m$	$\frac{1}{4}\frac{1}{4}\frac{1}{4}$	$\frac{3}{4}\frac{3}{4}\frac{3}{4}$	: 000	
Samarium	$R\bar{3}m$	$00w$	$00\bar{w}$	: 000	
Cadmium chloride	$R\bar{3}m$	$00w$	$00\bar{w}$	: 000	
Cadmium iodide	$P\bar{3}m1$	$\frac{1}{3}\frac{2}{3}w$	$\frac{2}{3}\frac{1}{3}\bar{w}$	: 000	
$m = 3\ n_t = 0\ n = 3$					
Selenium	$P3_121$	$u0\frac{1}{3}$	$0u\frac{2}{3}$	$\bar{u}\bar{u}0$	
$m = 3\ n_t = 2\ n = 4$					
DHCP	$P6_3/mmc$	$\frac{1}{3}\frac{2}{3}\frac{1}{4}$	$\frac{2}{3}\frac{1}{3}\frac{3}{4}$	: 000	$00\frac{1}{2}$
?Nickel arsenide	$P6_3/mmc$	$\frac{1}{3}\frac{2}{3}\frac{1}{4}$	$\frac{2}{3}\frac{1}{3}\frac{3}{4}$	: 000	$00\frac{1}{2}$
$m = 4\ n_t = 0\ n = 4$					
Graphite	$P6_3mc$	$\frac{1}{3}\frac{2}{3}0$	$\frac{2}{3}\frac{1}{3}\frac{1}{2}$	: 000	$00\frac{1}{2}$
Wurtzite	$P6_3mc$	$\frac{1}{3}\frac{2}{3}w$	$\frac{2}{3}\frac{1}{3}\frac{1}{2} + w$	: $\frac{1}{3}\frac{2}{3}0$	$\frac{2}{3}\frac{1}{3}0$
Nickel arsenide	$P6_3mc$	$\frac{1}{3}\frac{2}{3}w$	$\frac{2}{3}\frac{1}{3}\frac{1}{2} + w$	: 000	$00\frac{1}{2}$
Iodine/gallium	$Cmca$	$0vw$	$0\bar{v}\bar{w}$	$\frac{1}{2}v\frac{1}{2} - w$	$\frac{1}{2}\bar{v}\frac{1}{2} + w$
Lead oxide	$P4/nmm$	$0\frac{1}{2}w$	$\frac{1}{2}0\bar{w}$	: 000	$\frac{1}{2}\frac{1}{2}0$
β-Neptunium	$P42_12$	$0\frac{1}{2}w$	$\frac{1}{2}0\bar{w}$	: 000	$\frac{1}{2}\frac{1}{2}0$

highest symmetry. The structures are grouped according to values of m. It should be noted that the samarium and cadmium chloride structures as well as the double hexagonal close-packed and ?nickel arsenide structures differ only in that the atoms are identical in the first member of each pair but are different in the second. A doubt regarding the structure of nickel arsenide accounts for the two entries under this name.

Table 3. *The symmetry and form of the inner compliance tensor and the relative phase for crystal structures with* $m = 2$

Structure	Symmetry* of Σ	Σ	$\chi/2\pi$
Diamond Zincblende	$\bar{4}3m$	$\begin{bmatrix} . & . & . & a & . & . \\ . & . & . & . & a & . \\ . & . & . & . & . & a \end{bmatrix}$	$\frac{h+k+l}{4}$
HCP Tungsten carbide	$\bar{6}m2$	$\begin{bmatrix} . & . & . & . & . & 2a \\ a & -a & . & . & . & . \\ . & . & . & . & . & . \end{bmatrix}$	$\frac{h-k}{3}+\frac{l}{2}$
White tin	$\bar{4}m2$	$\begin{bmatrix} . & . & . & . & a & . \\ . & . & . & -a & . & . \\ b & -b & . & . & . & . \end{bmatrix}$	$\frac{2k+l}{4}$
α-Uranium	$m2m$	$\begin{bmatrix} . & . & . & . & . & a \\ b & c & d & . & . & . \\ . & . & . & e & . & . \end{bmatrix}$	$-2vk+\frac{l}{2}$
Arsenic	$3m$	$\begin{bmatrix} . & . & . & . & a & 2b \\ b & -b & . & a & . & . \\ c & c & d & . & . & . \end{bmatrix}$	$-2wl$

* Independent components: diamond, zincblende 1; HCP, tungsten carbide 1; white tin 2; α-uranium 5; arsenic 4.

Table 4. *The symmetry and forms of the inner compliance tensors and the relative phases for crystal structures with* $m = 3$

Structure	π	Symmetry* of Σ^π	$\chi^\pi/2\pi$
Fluorite	1	$\bar{4}3m$	$\frac{h+k+l}{2}$
	$\Sigma^1 = -2\Sigma^2$		
	2	$\bar{4}3m$	$\frac{h+k+l}{4}$
	$\Sigma^2 = \begin{bmatrix} . & . & . & a & . & . \\ . & . & . & . & a & . \\ . & . & . & . & . & a \end{bmatrix}$		
	3	$\bar{4}3m$	$-\frac{h+k+l}{4}$
	$\Sigma^3 = -\Sigma^2$		
Samarium Cadmium chloride	1	$3m$	$-2wl$
	$\Sigma^1 = -2\Sigma^2$		
	2	$3m$	wl
	$\Sigma^2 = \begin{bmatrix} . & . & . & . & a & . \\ . & . & . & a & . & . \\ b & b & c & . & . & . \end{bmatrix}$		
	3	$3m$	$-wl$
	$\Sigma^3 = -\Sigma^2$		

Table 4 (*cont.*)

Structure	π	Symmetry* of Σ^π	$\chi^\pi/2\pi$
Cadmium iodide	1	$3m$	$\frac{h-k}{3}-2wl$
	$\Sigma^1 = -2\Sigma^2$		
	2	$3m$	$\frac{h-k}{3}+wl$
	$\Sigma^2 = \begin{bmatrix} . & . & . & . & a & . \\ . & . & . & a & . & . \\ b & b & c & . & . & . \end{bmatrix}$		
	3	$3m$	$-\frac{h-k}{3}-wl$
	$\Sigma^3 = -\Sigma^2$		
Selenium	1	$m\perp(\mathbf{a}_1+\mathbf{a}_2)$	$-u(h-k)+\frac{l}{3}$
	$\Sigma^1 = \begin{bmatrix} c' & b' & d' & a' & -a'' & -(c''-b'') \\ -b'' & -c'' & -d'' & a'' & a' & (c'-b') \\ -e'' & e'' & . & -f'' & f' & 2e' \end{bmatrix}$		
	2	$m\perp\mathbf{a}_1$	$-u(h+2k)+\frac{l}{3}$
	$\Sigma^2 = \begin{bmatrix} . & . & . & . & a & c-b \\ b & c & d & -a & . & . \\ e & -e & . & f & . & . \end{bmatrix}$		
	3	$m\perp\mathbf{a}_2$	$-u(2h+k)-\frac{l}{3}$
	$\Sigma^3 = \begin{bmatrix} c' & b' & d' & a' & a'' & (c''-b'') \\ b'' & c'' & d'' & -a'' & a' & (c'-b') \\ e'' & -e'' & . & f'' & f' & 2e' \end{bmatrix}$		
	$p' = \sqrt{3}p/2,\ q'' = q/2$		
DHCP ?Nickel arsenide	1	$\bar{6}m2$	$\frac{h-k}{3}+\frac{l}{2}$
	$\Sigma^1 = -2\Sigma^2$		
	2	$3m$	$\frac{h-k}{3}+\frac{l}{4}$
	$\Sigma^2 = \begin{bmatrix} . & . & . & . & . & 2a \\ a & -a & . & . & . & . \\ . & . & . & . & . & . \end{bmatrix}$		
	3	$6/mmm$	$\frac{l}{2}$
	$\Sigma^3 = 0$		
	4	$3m$	$-\frac{h-k}{3}-\frac{l}{4}$
	$\Sigma^4 = -\Sigma^2$		
	5	$3m$	$\frac{h-k}{3}-\frac{l}{4}$
	$\Sigma^5 = \Sigma^2$		
	6	$3m$	$-\frac{h-k}{3}+\frac{l}{4}$
	$\Sigma^6 = -\Sigma^2$		

* Independent components: fluorite 1; samarium, cadmium chloride 3; cadmium iodide 3; selenium 6; DHCP, ?nickel arsenide 1.

4.1.1. *Structures with* $m = 2$. There is only one interlattice index ($\pi = 1$) in these structures and it may be omitted without ambiguity. The point symmetry of

the inner compliance tensor is deduced precisely as described in detail for the internal strain tensors in corundum (Cousins, 1981). The form of the tensor can now be taken either directly from Table 1 if the point symmetry corresponds to one of the standard settings or by transforming the entry in Table 1 if a variant setting is encountered. Examples of variant settings occur in white tin ($\bar{4}m2$ rather than $\bar{4}2m$) and in α-uranium where the diad is parallel to Ox_2 rather than Ox_3. The results are presented in Table 3. The relative phase χ is also listed.

4.1.2. *Structures with $m = 3$ and $m = 4$.* Tables 4 and 5 contain the results for the cases of $m = 3$ and $m = 4$ respectively. The same procedures are used as for $m = 2$ to determine the effect of crystal symmetry. There is now, however, the possibility of further simplification through geometrical conditions: $\Sigma^3 \equiv \Sigma^1 + \Sigma^2$ when $n = 3$ and $\Sigma^4 \equiv \Sigma^1 + \Sigma^2$, $\Sigma^5 \equiv \Sigma^2 + \Sigma^3$ and $\Sigma^6 \equiv \Sigma^1 + \Sigma^2 + \Sigma^3$ when $n = 4$. These relations of dependence also extend to the relative phases χ^π by virtue of definition.

5. Uniaxial stress derivatives of $|F(\mathbf{H})|^2$ in 20 simple structures

The determination of all components of the inner compliance tensors of a particular crystal will in

Table 5. *The symmetry and forms of the inner compliance tensors and the relative phases for crystal structures with $m = 4$*

Structure	π	Symmetry* of Σ^π	$\chi^\pi/2\pi$
Graphite	1	$\bar{6}m2$	$\frac{h-k}{3}+\frac{l}{2}$
	$\Sigma^1 = \begin{bmatrix} . & . & . & . & . & 4a \\ 2a & -2a & . & . & . & . \\ . & . & . & . & . & . \end{bmatrix}$		
	2	$3m$	$\frac{h-k}{3}+\frac{l}{2}$
	$\Sigma^2 = \begin{bmatrix} . & . & . & . & c & -2(a+b) \\ -(a+b) & (a+b) & . & c & . & . \\ d & d & e & . & . & . \end{bmatrix}$		
	3	$\bar{6}m2$	$\frac{l}{2}$
	$\Sigma^3 = \begin{bmatrix} . & . & . & . & . & 4b \\ 2b & -2b & . & . & . & . \\ . & . & . & . & . & . \end{bmatrix}$		
	4	$3m$	$-\frac{h-k}{3}$
	$\Sigma^4 = \Sigma^1 + \Sigma^2$		
	5	$3m$	$\frac{h-k}{3}$
	$\Sigma^5 = \Sigma^2 + \Sigma^3$		
	6	$3m$	$-\frac{h-k}{3}-\frac{l}{2}$
	$\Sigma^6 = \Sigma^1 + \Sigma^2 + \Sigma^3$		

Table 5 (*cont.*)

Structure	π	Symmetry* of Σ^π	$\chi^\pi/2\pi$
Wurtzite	1	$\bar{6}m2$	$\frac{h-k}{3}+\frac{l}{2}$
	$\Sigma^1 = \begin{bmatrix} . & . & . & . & . & 4a \\ 2a & -2a & . & . & . & . \\ . & . & . & . & . & . \end{bmatrix}$		
	2	$3m$	$-\frac{h-k}{3}-\frac{l}{2}-wl$
	$\Sigma^2 = \begin{bmatrix} . & . & . & . & c & -2(a+b) \\ -(a+b) & (a+b) & . & c & . & . \\ d & d & e & . & . & . \end{bmatrix}$		
	3	$\bar{6}m2$	$\frac{h-k}{3}+\frac{l}{2}$
	$\Sigma^3 = \begin{bmatrix} . & . & . & . & . & 4b \\ 2b & -2b & . & . & . & . \\ . & . & . & . & . & . \end{bmatrix}$		
	4	$3m$	$-wl$
	$\Sigma^4 = \Sigma^1 + \Sigma^2$		
	5	$3m$	$-wl$
	$\Sigma^5 = \Sigma^2 + \Sigma^3$		
	6	$3m$	$\frac{h-k}{3}+\frac{l}{2}-wl$
	$\Sigma^6 = \Sigma^1 + \Sigma^2 + \Sigma^3$		
Nickel arsenide	1	$\bar{6}m2$	$\frac{h-k}{3}+\frac{l}{2}$
	$\Sigma^1 = \begin{bmatrix} . & . & . & . & . & 4a \\ 2a & -2a & . & . & . & . \\ . & . & . & . & . & . \end{bmatrix}$		
	2	$3m$	$\frac{h-k}{3}+\frac{l}{2}-wl$
	$\Sigma^2 = \begin{bmatrix} . & . & . & . & c & -2(a+b) \\ -(a+b) & (a+b) & . & c & . & . \\ d & d & e & . & . & . \end{bmatrix}$		
	3	$\bar{6}m2$	$\frac{l}{2}$
	$\Sigma^3 = \begin{bmatrix} . & . & . & . & . & 4b \\ 2b & -2b & . & . & . & . \\ . & . & . & . & . & . \end{bmatrix}$		
	4	$3m$	$-\frac{h-k}{3}-wl$
	$\Sigma^4 = \Sigma^1 + \Sigma^2$		
	5	$3m$	$\frac{h-k}{3}-wl$
	$\Sigma^5 = \Sigma^2 + \Sigma^3$		
	6	$3m$	$-\frac{h-k}{3}-\frac{l}{2}-wl$
	$\Sigma^6 = \Sigma^1 + \Sigma^2 + \Sigma^3$		

* Independent components: graphite 5; wurtzite 5; nickel arsenide 5.

Table 5 (*cont.*)

Structure	π	Symmetry* of Σ^π	$\chi^\pi/2\pi$
Iodine/gallium	1	$m \perp 0x_1$	$-2vk - 2wl$
	$\Sigma^1 = \Sigma^4 - \Sigma^2$		
	2	$m2m$	$\frac{h+l}{2} + 2vk$
	$\Sigma^2 = \begin{bmatrix} . & . & . & . & . & a \\ b & c & d & . & . & . \\ . & . & . & e & . & . \end{bmatrix}$		
	3	$m \perp 0x_1$	$-2vk + 2wl$
	$\Sigma^3 = -(\Sigma^4 + \Sigma^2)$		
	4	$mm2$	$\frac{h+l}{2} - 2wl$
	$\Sigma^4 = \begin{bmatrix} . & . & . & . & f & . \\ . & . & . & g & . & . \\ h & i & j & . & . & . \end{bmatrix}$		
	5	$mm2$	$\frac{h+l}{2} + 2wl$
	$\Sigma^5 = -\Sigma^4$		
	6	$m2m$	$\frac{h+l}{2} - 2vk$
	$\Sigma^6 = -\Sigma^2$		
Lead oxide	1	$4mm$	$\frac{h+k}{2} - 2wl$
	$\Sigma^1 = \begin{bmatrix} . & . & . & . & 2a & . \\ . & . & . & 2a & . & . \\ 2b & 2b & 2c & . & . & . \end{bmatrix}$		
	2	$mm2$	$\frac{h}{2} + wl$
	$\Sigma^2 = \begin{bmatrix} . & . & . & . & . & -(a+d) & . \\ . & . & . & . & d-a & . & . \\ -(b+e) & (e-b) & -c & . & . & . & . \end{bmatrix}$		
	3	$\bar{4}m2$	$\frac{h+k}{2}$
	$\Sigma^3 = \begin{bmatrix} . & . & . & . & 2d & . \\ . & . & . & -2d & . & . \\ 2e & -2e & . & . & . & . \end{bmatrix}$		
	4	$mm2$	$\frac{k}{2} - wl$
	$\Sigma^4 = \begin{bmatrix} . & . & . & . & a-d & . \\ . & . & . & a+d & . & . \\ b-e & b+e & c & . & . & . \end{bmatrix}$		
	5	$mm2$	$\frac{k}{2} + wl$
	$\Sigma^5 = -\Sigma^4$		
	6	$mm2$	$\frac{h}{2} - wl$
	$\Sigma^6 = -\Sigma^2$		

Table 5 (*cont.*)

Structure	π	Symmetry* of Σ^π	$\chi^\pi/2\pi$
β-Neptunium	1	$4mm$	$\frac{h+k}{2} - 2wl$
	$\Sigma^1 = \begin{bmatrix} . & . & . & . & 2a & . \\ . & . & . & 2a & . & . \\ 2b & 2b & 2c & . & . & . \end{bmatrix}$		
	2	$2 \parallel Ox_3$	$\frac{h}{2} + wl$
	$\Sigma^2 = \begin{bmatrix} . & . & . & f & d-a & . \\ . & . & . & -(a+d) & -f & . \\ -(b+e) & (e-b) & -c & . & . & . \end{bmatrix}$		
	3	$\bar{4}m2$	$\frac{h+k}{2}$
	$\Sigma^3 = \begin{bmatrix} . & . & . & . & 2d & . \\ . & . & . & -2d & . & . \\ 2e & -2e & . & . & . & . \end{bmatrix}$		
	4	$2 \parallel Ox_3$	$\frac{k}{2} - wl$
	$\Sigma^4 = \begin{bmatrix} . & . & . & f & a+d & . \\ . & . & . & a-d & -f & . \\ b-e & b+e & c & . & . & . \end{bmatrix}$		
	5	$2 \parallel Ox_3$	$\frac{k}{2} + wl$
	$\Sigma^5 = \begin{bmatrix} . & . & . & f & -(a+d) & . \\ . & . & . & d-a & -f & . \\ e-b & -(b+e) & -c & . & . & . \end{bmatrix}$		
	6	$2 \parallel Ox_3$	$\frac{h}{2} - wl$
	$\Sigma^6 = \begin{bmatrix} . & . & . & f & a-d & . \\ . & . & . & a+d & -f & . \\ b+e & b-e & c & . & . & . \end{bmatrix}$		

* Independent components: iodine/gallium 10; lead oxide 5; β-neptunium 6.

general require the values of $\mathrm{d}|F(\mathbf{H})|^2/\mathrm{d}\sigma$ for a number of reflections and various axes of stress. These stress derivatives depend on $\psi_{\mathbf{H}}^\pi$ and (26) and (27) show that the different $\psi_{\mathbf{H}}^\pi$ in a particular structure are coupled by relative phase terms ($\sin \chi_{\mathbf{H}}^\pi$ or $\cos \psi_{\mathbf{H}}^\pi$) as well as by quadratic terms in the form factors. The choice of reflections and stress axes is most easily discussed in connection with structures for which $m = 2$.

5.1. *Structures with* $m = 2$

In terms of the inner compliance tensor, (28) may be written

$$\psi_{\mathbf{H}} = 2\pi\sigma[h_1\, h_2\, h_3]\begin{bmatrix} \Sigma_{11} & \Sigma_{12} & \Sigma_{13} & \Sigma_{14} & \Sigma_{15} & \Sigma_{16} \\ \Sigma_{21} & \Sigma_{22} & \Sigma_{23} & \Sigma_{24} & \Sigma_{25} & \Sigma_{26} \\ \Sigma_{31} & \Sigma_{32} & \Sigma_{33} & \Sigma_{34} & \Sigma_{35} & \Sigma_{36} \end{bmatrix}\begin{bmatrix} l_1^2 \\ l_2^2 \\ l_3^2 \\ l_2 l_3 \\ l_3 l_1 \\ l_1 l_2 \end{bmatrix} \tag{31}$$

If both $\mathbf{h}$ and $\mathbf{l}$ lie along coordinate axes then $\psi_{\mathbf{H}}$ depends solely on a single Σ_{iJ} component from the first three columns. For example, if $\mathbf{h} = [h_1 00]$ and $\mathbf{l} = [010]$ then $\psi_{\mathbf{H}} = 2\pi\sigma h_1 \Sigma_{12}$. Elements in the second three columns can be isolated by observing a particular reflection under two distinct stress axes: if $\mathbf{h} = [h_1 00]$ and $\mathbf{l}^{\pm} = [l_1, \pm l_2, 0]$ then $\psi_{\mathbf{H}}^{\pm} = 2\pi\sigma h_1(\Sigma_{11} l_1^2 + \Sigma_{12} l_2^2 \pm \Sigma_{16} l_1 l_2)$ from which, by subtraction, Σ_{16} may be isolated.

The presence of the relative phase $\chi_{\mathbf{H}}$ causes possible reflections to be divided into different classes. In Table 6 are presented the specific forms of $\sigma\, \mathrm{d}|F(\mathbf{H})|^2/\mathrm{d}\sigma$ and $|F(\mathbf{H})|_0^2$ for these different classes for each of the structures with $m = 2$. When there are ν lattice points in the unit cell the values of $|F(\mathbf{H})|_0^2$ and its derivatives must be multiplied by ν^2. This is included in the table and indicates that for arsenic a hexagonal cell (three lattice points) has been preferred to the primitive rhombohedral cell.

In certain structures it will be seen that $|F(\mathbf{H})|_0^2$ is zero for certain reflection classes. This occurs when the structure is non-symmorphic (*i.e.* it contains screw axes and/or glide planes). These are sometimes strictly forbidden (*e.g.* 002 in diamond) or weakly allowed (*e.g.* 222 in diamond). In the latter case the appearance of the reflection indicates an aspherical electron distribution and anisotropic and anharmonic atomic motions. Measurements on strictly forbidden reflections are useful because the induced reflection is totally due to the application of stress.

5.2. *Structures with $m = 3$ and $m = 4$*

Tables 7 and 8 contain the same kind of information as Table 6 but for structures with $m = 3$ and $m = 4$. In Table 8 there are certain reflections where the stress derivatives of $|F(\mathbf{H})|^2$ involve a complicated quadratic function of the $\psi_{\mathbf{H}}^{\pm}$. These are unlikely to be of value in the determination of the inner compliance tensors and have been omitted, their absence being denoted by the letter Q.

6. Concluding remarks

The inner compliance tensors and the internal strain tensors of crystals with 2, 3 or 4 atoms per lattice point may be determined by observing the uniaxial stress dependence of the intensity of selected reflections.

Table 6. *$|F(\mathbf{H})|_0^2$ and $\sigma\, \mathrm{d}|F(\mathbf{H})|^2/\mathrm{d}\sigma$ for structures with $m = 2$*

Structure	Reflection conditions		$\lvert F(\mathbf{H})\rvert_0^2$	$\sigma\, \mathrm{d}\lvert F(\mathbf{H})\rvert^2/\mathrm{d}\sigma$	
Diamond	$h+k+l$	$=4n$	$64f^2$		$-32f^2(\psi)^2$
		$4n \pm 1$	$32f^2$	$\mp 32f^2\psi$	
		$4n+2$	0		$32f^2(\psi)^2$
Zincblende	$h+k+l$	$=4n$	$16(f_1+f_2)^2$		$-32f_1f_2(\psi)^2$
		$4n \pm 1$	$16(f_1^2+f_2^2)$	$\mp 32f_1f_2\psi$	
		$4n+2$	$16(f_1-f_2)^2$		$32f_1f_2(\psi)^2$
HCP	$h-k=3m$,	$l=2n$	$4f^2$		$-2f^2(\psi)^2$
		$2n+1$	0		$2f^2(\psi)^2$
	$3m \pm 1$	$2n$	f^2	$\mp\sqrt{3}f^2\psi$	
		$2n+1$	$3f^2$	$\pm\sqrt{3}f^2\psi$	
Tungsten carbide	$h-k=3m$,	$l=2n$	$(f_1+f_2)^2$		$-2f_1f_2(\psi)^2$
		$2n+1$	$(f_1-f_2)^2$		$2f_1f_2(\psi)^2$
	$3m \pm 1$	$2n$	$f_1^2+f_2^2-f_1f_2$	$\mp\sqrt{3}f_1f_2\psi$	
		$2n+1$	$f_1^2+f_2^2+f_1f_2$	$\pm\sqrt{3}f_1f_2\psi$	
White tin	$2k+l$	$=4n$	$16f^2$		$-8f^2(\psi)^2$
		$4n \pm 1$	$8f^2$	$\mp 8f^2\psi$	
		$4n+2$	0		$8f^2(\psi)^2$
α-Uranium	$k=0$	$l=2n$	$16f^2$		$-8f^2(\psi)^2$
		$2n+1$	0		$8f^2(\psi)^2$
	$\neq 0$	$2n$	$8f^2(1+\cos 2\theta)$	$8f^2\sin 2\theta\psi$	
		$2n+1$	$8f^2(1-\cos 2\theta)$	$-8f^2\sin 2\theta\psi$	
$\theta = 2\pi vk$					
Arsenic	$l=0$		$36f^2$		$-18f^2(\psi)^2$
	$l\neq 0$		$18f^2(1+\cos 2\theta)$	$18f^2\sin 2\theta\psi$	
$\theta = 2\pi wl$					

Table 7. $|F(\mathbf{H})|_0^2$ *and* $\sigma\,\mathrm{d}|F(\mathbf{H})|^2/\mathrm{d}\sigma$ *for structures with* $m = 3$

Structure	Reflection conditions		$\lvert F(\mathbf{H})\rvert_0^2$	$\sigma\,\mathrm{d}\lvert F(\mathbf{H})\rvert^2/\mathrm{d}\sigma$	
Fluorite	$h+k+l$	$=4n$	$16(2f_1+f_3)^2$		$-64f_1(2f_1+f_3)(\psi^2)^2$
		$4n\pm1$	$16f_3^2$	$\mp64f_1f_3\psi^2$	
		$4n+2$	$16(2f_1-f_3)^2$		$-64f_1(2f_1-f_3)(\psi^2)^2$
Samarium	$l=0$		$81f^2$		$-108f^2(\psi^2)^2$
	$l\neq0$		$9f^2(1+2\cos\theta)^2$	$-36f^2\sin\theta(1+2\cos\theta)\psi^2$	
$\theta=2\pi wl$					
Cadmium chloride	$l=0$		$9(2f_1+f_3)^2$		$-36f_1(2f_1+f_3)(\psi^2)^2$
	$l\neq0$		$9(2f_1\cos\theta+f_3)^2$	$-36f_1\sin\theta(2f_1\cos\theta+f_3)\psi^2$	
$\theta=2\pi wl$					
Cadmium iodide	$h-k=3m$,	$l=0$	$(2f_1+f_3)^2$		$-4f_1(2f_1+f_3)(\psi^2)^2$
		$\neq0$	$(2f_1\cos\theta+f_3)^2$	$-4f_1\sin\theta(2f_1\cos\theta+f_3)\psi^2$	
	$3m\pm1$	$=0$	$(f_1-f_3)^2$	$\pm2\sqrt{3}f_1(f_1-f_3)\psi^2$	
		$\neq0$	$[f_1(\cos\theta\pm\sqrt{3}\sin\theta)-f_3]^2$	$2f_1\{(f_1\sin2\theta+f_3\sin\theta)$ $\pm\sqrt{3}(f_1\cos2\theta-f_3\cos\theta)\}\psi^2$	
$\theta=2\pi wl$					
Selenium	$h=k=0$	$l=3n$	$9f^2$		$-2f^2\{(\psi^1)^2+(\psi^2)^2+(\psi^3)^2\}$
		$3n\pm1$	0		$f^2\{(\psi^1)^2+(\psi^2)^2+(\psi^3)^2\}$
	$h=k\neq0$	$l=3n$	$f^2(5+4\cos3\theta)$	$2f^2\sin3\theta(\psi^2+\psi^3)$	
	$h=-2k\neq0$		$f^2(5+4\cos3\varphi)$	$-2f^2\sin3\varphi(\psi^3+\psi^1)$	
	$2h=-k\neq0$		$f^2(5+4\cos3\theta)$	$2f^2\sin3\theta(\psi^1-\psi^2)$	
	$h=k\neq0$	$3n\pm1$	$2f^2(1-\cos3\theta)$	$-f^2\{\sin3\theta(\psi^2+\psi^3)$ $\pm\sqrt{3}(1-\cos3\theta)\psi^1\}$	
	$h=-2k\neq0$		$2f^2(1-\cos3\varphi)$	$f^2\{\sin3\varphi(\psi^3+\psi^1)$ $\mp\sqrt{3}(1-\cos3\varphi)\psi^2\}$	
	$2h=-k\neq0$		$2f^2(1-\cos3\theta)$	$-f^2\{\sin3\theta(\psi^1-\psi^2)$ $\mp\sqrt{3}(1-\cos3\theta)\psi^3\}$	
$\theta=2\pi uh$ $\varphi=2\pi uk$					
DHCP	$h-k=3m$	$l=4n$	$16f^2$		$-16f^2(\psi^2)^2$
		$4n\pm1$	0		$8f^2(\psi^2)^2$
		$4n+2$	0		0
	$3m\pm1$	$4n$	f^2	$\mp2\sqrt{3}f^2\psi^2$	
		$4n\pm1$	$3f^2$	$\mp2\sqrt{3}f^2\psi^{2*}$	
		$4n+2$	$9f^2$	$\pm6\sqrt{3}f^2\psi^2$	
?Nickel arsenide	$h-k=3m$	$l=4n$	$4(f_1+f_3)^2$		$-8f_1(f_1+f_3)(\psi^2)^2$
		$4n\pm1$	0		$8f_1^2(\psi^2)^2$
		$4n+2$	$4(f_1-f_3)^2$		$-8f_1(f_1-f_3)(\psi^2)^2$
	$3m\pm1$	$4n$	$(f_1-2f_3)^2$	$\pm2\sqrt{3}f_1(f_1-2f_3)\psi^2$	
		$4n\pm1$	$3f_1^2$	$\mp2\sqrt{3}f_1^2\psi^{2*}$	
		$4n+2$	$(f_1+2f_3)^2$	$\pm6\sqrt{3}f_1(f_1+2f_3)\psi^2$	

* Alternative sign comes from the l condition.

Increasing complexity of expressions for this dependence, already evident in Table 8, suggests that structures with five or more atoms per lattice point will require a different type of investigation. One possibility would be the automatic collection of a large number of reflections from the stressed crystal in a structure-determination configuration. The changes in $|F(\mathbf{H})|^2$ on going from the unstressed to the stressed crystal could then be made to yield the components of the inner compliance tensors by an optimization procedure.

Only three materials have so far had their internal strain tensors determined. Silicon and germanium were first investigated by Segmüller (1963, 1964) and Segmüller & Neyer (1965) and recently by Cousins, Gerward, Nielsen *et al.* (1982), Cousins, Gerward, Staun Olsen *et al.* (1982) and (Si only) by d'Amour, Denner, Schulz & Cardona (1982). For both materials the single dimensionless internal strain parameter $\bar{A}$ has the magnitude ~0·18 and is accurate to about 5%. Gallium arsenide was investigated by Koumelis & Rozis (1975) and by Koumelis, Zardas, Londos & Leventouri (1976). Their result corresponds to $|\bar{A}| \simeq 0{\cdot}19$, although a reanalysis of their data, undertaken as a preliminary to planned work on III–V compounds, suggests that the figure should be higher.

In the meantime there is a great opportunity for work on crystals belonging to the 20 structures described in this paper. Two considerations make such work desirable. Firstly, the internal strain tensors are potentially of great value in the assessment of models of bonding and cohesion where they take their place alongside the ordinary elastic constants. Secondly, there are many experiments performed where uniaxial stress is used to remove a degeneracy or probe some

Table 8. $|F(\mathbf{H})|_0^2$ *and* $\sigma\,\mathrm{d}|F(\mathbf{H})|^2/\mathrm{d}\sigma$ *for structures with* $m = 4$

The letter Q indicates the omission of a complicated quadratic expression

Structure	Reflection conditions		$\lvert F(\mathbf{H})\rvert_0^2$	$\sigma\,\mathrm{d}\lvert F(\mathbf{H})\rvert^2/\mathrm{d}\sigma$	
Graphite	$h-k=3m$	$l=2n$	$16f^2$		Q
		$2n+1$	0		$2f^2(\psi^1+\psi^3)^2$
	$3m\pm1$	$2n$	f^2	$\pm\sqrt{3}f^2\psi^1$	
		$2n+1$	$3f^2$	$\pm\sqrt{3}f^2(\psi^1-2\psi^3)$	
Wurtzite	$h-k=3m$	$l=2n$	$4(f_1^2+f_3^2+2f_1f_3\cos\theta)$	$4f_1f_3\sin\theta(\psi^1+2\psi^2+\psi^3)$	
		$2n+1$	0		$2\{f_1^2(\psi^1)^2+f_3^2(\psi^3)^2+2f_1f_3\cos\theta\psi^1\psi^3\}$
	$3m\pm1$	$2n$	$f_1^2+f_3^2+2f_1f_3\cos\theta$	$f_1f_3\sin\theta(\psi^1+2\psi^2+\psi^3)\mp\sqrt{3}[f_1^2\psi^1+f_3^2\psi^3+f_1f_3\cos\theta(\psi^1+\psi^3)]$	
		$2n+1$	$3(f_1^2+f_3^2+2f_1f_3\cos\theta)$	$3f_1f_3\sin\theta(\psi^1+2\psi^2+\psi^3)\pm\sqrt{3}[f_1^2\psi^1+f_3^2\psi^3+f_1f_3\cos\theta(\psi^1+\psi^3)]$	
$\theta=2\pi wl$					
Nickel arsenide	$h-k=3m$	$l=0$	$4(f_1+f_3)^2$		Q
		$2n\neq0$	$4(f_1^2+f_3^2+2f_1f_3\cos\theta)$	$4f_1f_3\sin\theta(\psi^1+2\psi^2+\psi^3)$	
		$2n+1$	0		$2\{f_1^2(\psi^1)^2+f_3^2(\psi^3)^2+2f_1f_3\cos\theta\psi^1\psi^3\}$
	$3m\pm1$	0	$(f_1-2f_3)^2$	$\mp\sqrt{3}f_1(f_1-2f_3)\psi^1$	
		$2n\neq0$	$f_1^2+4f_3^2-4f_1f_3\cos\theta$	$-2f_1f_3\sin\theta(\psi^1+2\psi^2+\psi^3)\mp\sqrt{3}f_1(f_1-2f_3\cos\theta)\psi^1$	
		$2n+1$	$3f_1^2$	$\pm\sqrt{3}f_1(f_1\psi^1-2f_3\cos\theta\psi^3)$	
$\theta=2\pi wl$					
Iodine/gallium	$l=0$ $k=0$	$h=2n$	$64f^2$		$-8f^2[(\psi^2)^2+(\psi^4)^2]$
		$2n+1$	0		0
	$\neq0$	$2n$	$32f^2(1+\cos2\theta_2)$	$-8f^2\sin2\theta_2\,\psi^2$	
		$2n+1$	0		$4f^2(1-\cos2\theta_2)(\psi^4)^2$
	$\neq0$ $=0$	$h+l=2n$	$32f^2(1+\cos2\theta_3)$	$8f^2\sin2\theta_3\,\psi^4$	
		$2n+1$	0		$4f^2(1-\cos2\theta_3)(\psi^2)^2$
	$\neq0$	$2n$	$16f^2(1+\cos2\theta_2)(1+\cos2\theta_3)$	$-4f^2\{\sin2\theta_2(1+\cos2\theta_3)\psi^2-\sin2\theta_3(1+\cos2\theta_2)\psi^4\}$	
		$2n+1$	$16f^2(1-\cos2\theta_2)(1-\cos2\theta_3)$	$4f^2\{\sin2\theta_2(1-\cos2\theta_3)\psi^2-\sin2\theta_3(1-\cos2\theta_2)\psi^4\}$	
$\theta_2=2\pi vk$, $\theta_3=2\pi wl$					
Lead oxide	$h=2m$ $k=2n$	$l=0$	$4(f_1+f_3)^2$		Q
	$2m+1$ $2n+1$		$4(f_1-f_3)^2$		Q
	$2m$ $2n$	$\neq0$	$4(f_1\cos\theta+f_3)^2$	$-4f_1\sin\theta(f_1\cos\theta+f_3)(\psi^2-\psi^4)$	
	$2n+1$		$4f_1^2\sin^2\theta$	$4f_1\sin\theta\{(f_1\cos\theta-f_3)\psi^2-(f_1\cos\theta+f_3)\psi^4\}$	
	$2m+1$ $2n$		$4f_1^2\sin^2\theta$	$4f_1\sin\theta\{(f_1\cos\theta+f_3)\psi^2-(f_1\cos\theta-f_3)\psi^4\}$	
	$2n+1$		$4(f_1\cos\theta-f_3)^2$	$-4f_1\sin\theta(f_1\cos\theta-f_3)(\psi^2-\psi^4)$	
$\theta=2\pi wl$					
β-Neptunium	$h=2m$ $k=2n$	$l=0$	$16f^2$		Q
	$2n+1$		0		$2f^2(\psi^1-\psi^3)^2$
	$2m+1$ $2n$		0		$2f^2(\psi^1+\psi^3)^2$
	$2n+1$		0		Q
	$2m$ $2n$	$\neq0$	$4f^2(1+\cos\theta)^2$	$4f^2\sin\theta(1+\cos\theta)\psi^1$	
	$2n+1$		$4f^2\sin^2\theta$	$-4f^2\sin\theta(\cos\theta\psi^1-\psi^3)$	
	$2m+1$ $2n$		$4f^2\sin^2\theta$	$-4f^2\sin\theta(\cos\theta\psi^1+\psi^3)$	
	$2n+1$		$4f^2(1-\cos\theta)^2$	$-4f^2\sin\theta(1-\cos\theta)\psi^1$	
$\theta=2\pi wl$					

phenomenon. In such cases the actual movements of sublattices is crucial to understanding the observations. These movements canot be deduced from macroscopic elasticity alone and recourse must be had to internal strain tensors.

I am grateful for a period as Guest Professor at Physics Laboratory II, H. C. Ørsted Institute, Copenhagen University during which part of this work was completed.

References

AMOUR, H. D', DENNER, W., SCHULZ, H. & CARDONA, M. (1982). *J. Appl. Cryst.* **15**, 148–153.

COUSINS, C. S. G. (1978*a*). *J. Phys. C*, **11**, 4867–4879.

COUSINS, C. S. G. (1978*b*). *J. Phys. C*, **11**, 4881–4900.

COUSINS, C. S. G. (1981). *J. Phys. C*, **14**, 1585–1602.

COUSINS, C. S. G., GERWARD, L., NIELSEN, K., STAUN OLSEN, J., SELSMARK, B., SHELDON, B. J. & WEBSTER, G. E. (1982). *J. Phys. C*, **15**, L651–L654.

COUSINS, C. S. G., GERWARD, L., STAUN OLSEN, J., SELSMARK, B. & SHELDON, B. J. (1982). *J. Appl. Cryst.* **15**, 154–159.
GALASSO, F. (1970). *Structure and Properties of Inorganic Solids*. Oxford: Pergamon.
KOUMELIS, C. N. & ROZIS, E. K. (1975). *Acta Cryst.* A**31**, 84–87; erratum: *Acta Cryst.* (1976). A**32**, 170.
KOUMELIS, C. N., ZARDAS, G. E., LONDOS, C. A. & LEVENTOURI, D. K. (1976). *Acta Cryst.* A**32**, 306–311.
NYE, J. F. (1957). *Physical Properties of Crystals*. Oxford: Clarendon Press.
SEGMÜLLER, A. (1963). *Phys. Lett.* **4**, 277–278.
SEGMÜLLER, A. (1964). *Phys. Kondens. Mater.* **3**, 18–28.
SEGMÜLLER, A. & NEYER, H. R. (1965). *Phys. Kondens. Mater.* **4**, 63–70.
SLATER, J. C. (1965). *Quantum Theory of Molecules and Solids*, Vol. 2. New York: McGraw-Hill.

SHORT COMMUNICATIONS

Contributions intended for publication under this heading should be expressly so marked; they should not exceed about 1000 *words; they should be forwarded in the usual way to the appropriate Co-editor; they will be published as speedily as possible.*

Acta Cryst. (1983). A**39**, 268–269

On the atomic scattering factor for O^{2-}.

By E. HOVESTREYDT, *Laboratoire de Cristallographie aux Rayons X, Université de Genève, 24 quai Ernest Answermet, CH-1211 Genève 4, Switzerland*

(*Received* 26 *August* 1982; *accepted* 23 *September* 1982)

Abstract

The sin θ/λ dependence of the scattering factor for O^{2-} is approximated by the generally used exponential expression using nine coefficients. The corresponding fit is better than either of the two based upon the functions proposed by Tokonami.

A comparison of the theoretical O^{2-} form factor with experimental measurement by Raccah & Arnott (1967) indicates that the atomic scattering factor for O^{2-} given by Tokonami (1965) is a reasonable one.* The factor is based on calculations by Yamashita [1964, cited by Tokonami (1965)] who used the 1*s* and 2*s* wave functions of Watson (1958) for oxygen in a +1 well and derived the 2*p* function by a variational principle.

The analytical expressions (one for the Cu $K\alpha$ range and one for the Mo $K\alpha$ range) suggested by Tokonami (1965) yield, however, a poor fit. It was therefore decided to develop a better analytical expression based on the generally used fitting curve with nine coefficients.

Results

The nine coefficients for the expression

$$\sum_{i=1}^{4} a_i e^{-b_i \sin^2\theta/\lambda^2} + c$$

were obtained by a least-squares routine. Use was made of the E04HFE program of the *NAG Library* (1978) which is based on a Gauss–Newton algorithm for finding a minimum of a sum of squares of non-linear functions. As starting values the coefficients for O, tabulated in *International Tables for X-ray Crystallography* (1974), were supplied.

Table 1 contains the coefficients, calculated by the program, and Table 2 gives a comparison between (*a*)

Table 1. *The nine coefficients of the analytical expression* $\sum_{i=1}^{4} e^{-b_i \sin^2\theta/\lambda^2} + c$ *for the* O^{2-} *form factor*

a_1	3·75040	b_1	16·5151	c	0·242060
a_2	2·84294	b_2	6·59203		
a_3	1·54298	b_3	0·319201		
a_4	1·62091	b_4	43·3486		

Table 2. *Comparison between the different fitting curves and the scattering factor* (f) *of* O^{2-}

sin θ/λ	f	Fit (present work)	Fit Cu $K\alpha$ range (Tokonami)	Fit Mo $K\alpha$ range (Tokonami)
0·00	10·000	9·999	9·99	9·93
0·05	9·633	9·633	9·63	9·61
0·10	8·671	8·672	8·69	8·72
0·15	7·423	7·423	7·43	7·50
0·20	6·174	6·173	6·17	6·21
0·25	5·081	5·081	5·07	5·05
0·30	4·192	4·193	4·19	4·12
0·35	3·498	3·498	3·51	3·44
0·40	2·968	2·967	2·98	2·95
0·50	2·274	2·274	2·27	2·33
0·60	1·891	1·892	1·88	1·94
0·70	1·676	1·675	–	1·67
0·80	1·543	1·542	–	1·49
0·90	1·447	1·447	–	1·38
1·00	1·367	1·367	–	1·32
1·10	1·291	1·292	–	1·29
1·20	1·216	1·217	–	1·28
1·30	1·142	1·142	–	1·27
1·50	0·995	0·994	–	–
1·70	0·856	0·855	–	–
1·90	0·729	0·729	–	–

* Various other calculations are known (Schwarz & Schulz, 1978; Schmidt & Weiss, 1979; Schmidt, Sen & Weiss, 1980), but it is beyond the scope of this paper to compare them.

0567-7394/83/020268-02$01.50